



## A Novel Method for The Preparation of Conductive Methyl Cellulose-Silver Nanoparticles-Polyaniline-Nanocomposite



Manal A. El-Sheikh<sup>1,2\*</sup>, Amal A. Al-Enezy<sup>1</sup>, Fatema Z. El-Enezy<sup>1</sup>, Dalil K. El-Shammri<sup>1</sup>, Fatem M. El-Enezy<sup>1</sup>, Waad F. Al-Rowili<sup>1</sup>

<sup>1</sup>Chemistry Department, College of Science and Arts, AlQurayyat, Jouf University, Kingdom of Saudi Arabia

<sup>2</sup>Pretreatment and Finishing of Cellulosic Fibers Department, Textile Research Division, National Research Centre, Egypt.

**A** NOVEL green method for the synthesis of conductive nanocomposite -using silver nitrate, methyl cellulose (MC), glycerol, and aniline- was adopted. Here, silver nitrate was used as a precursor, methyl cellulose as both reducing and capping agent, glycerol as a co-reducing and ductility agent and water as solvent. While silver nitrate oxidizes aniline to polyaniline, it is reduced to silver nanoparticles. Doing so, both conductive polyaniline and conductive silver nanoparticle were in-situ synthesized via the formation of methyl cellulose-silver-polyaniline nanocomposite. Reproducibility of the nanocomposite revealed that the synthesis process is consistent. The nanocomposite film was characterized by FTIR, SEM, EDAX, XRD, and conductivity. XRD pattern showed poly crystallinity. TEM of the colloidal solution showed different particle shapes of AgNPs with size from 4-36 nm and d-spacing of 0.22 nm. SAED exhibits ring pattern with bright spots displaying polycrystallinity. Nanocomposite film, coated glass, cotton and polyester fabrics showed promising conductivity.

**Keywords:** Silver nanoparticles, Polyaniline, Glycerol, Methyl Cellulose, Polycrystallinity, d spacing.

### Introduction

Recently, metal nanoparticles have become one of the most important chemical products due to their different important applications in health, textiles, pharmaceutical, cosmetics, energy, ... etc. As a result, there is a global cause of concern in research to synthesize metal nanoparticles using green tools. Among the green methods used in the synthesis of metal nanoparticles are the use of phytochemicals [1], Enzymes, bacteria, and biopolymers [2-17]. All are used as both reducing and capping agent in the synthesis of metal nanoparticles.

Silver nanoparticles (AgNPs) were synthesized using different green methods. Renewable, biodegradable, eco-friendly biopolymers containing hydroxyl groups were used as both

reducing and capping agent. Among these biopolymers, starch [3-6, 8, 9, 12, 18], chitosan [19, 20] cellulose [7, 21-23] and their derivatives showed powerful biopolymers for effective green preparation of AgNPs.

Aniline have been oxidized to polyaniline (PANi) using silver nitrate [24] or silver wire [14, 25]. Subsequently, Ag<sup>+</sup> ions are reduced to AgNPs [24, 26-34]. Doing so, both conductive PANi and conductive AgNps are produced. These conductive materials can be used for coating non-conductive fabrics to impart conductive properties. Polyaniline grafted chitosan or cellulose copolymers were prepared by the chemical in situ polymerization of aniline while AgNPs were synthesized by chemical reduction method and incorporated into the polymer matrix or by in situ polymerization of aniline monomer

\*Corresponding author e-mail: melsheikh@ju.edu.sa

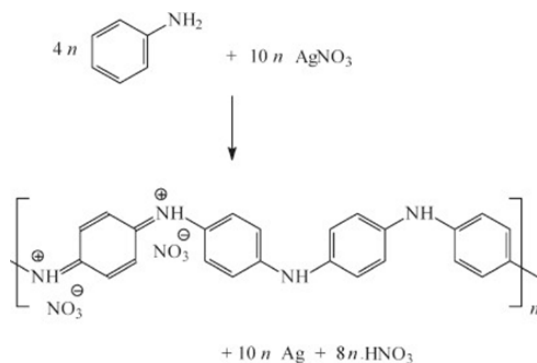
ORCID ID: <https://orcid.org/0000-0001-5148-5755>

Received 4/4/2020; Accepted 12/4/2020

DOI: 10.21608/ejchem.2020.27264.2568

©2020 National Information and Documentation Center (NIDOC)

containing silver nitrate [35-38]. Equation 1 shows the reaction between aniline and silver nitrate. Aniline is oxidized with silver nitrate to PANi and metallic silver. Nitric acid is a byproduct. An acidic medium is necessary [27].



**Equation 1: Reaction between aniline and silver nitrate [27]**

Conducting polymers have generated a great deal of interest because of their physical and chemical properties as well as their potential in industrially useful materials [39] such as applications of polymers in solar cells [40], fuel cell [41], sensing urea [42], surface-conductive glass fibers [43], water treatment [44], smart textiles [4, 45-51], conducting paper [39, 52], conductive wood [53] and conductive cellulose acetate membrane [54, 55].

As a polyol, glycerol can be used as reducing agent for the reduction of  $\text{Ag}^+$  to  $\text{Ag}^0$ . Glycerol was recently used as a reducing agent in the synthesis of AgNPs [56-59]. An anhydrous glycerol colloid containing nano-silver was synthesized for the first time with heating and stirring method by using silver nitrate ( $\text{AgNO}_3$ ) as silver source, anhydrous glycerol as reducing agent and dispersion medium [56, 59]. Glycerol acted also as a co-solvent and co-surfactant to equilibrate the hydrophilic and hydrophobic proximities in the synthesis of curcumin capped AgNPs [60].

In this research, a novel method for polymerizing aniline in the presence of methyl cellulose (MC), glycerol and silver nitrate has been developed. While silver ions are reduced to AgNPs, aniline is oxidized to PANi. Both PANi and AgNPs are conductive materials that are finally produces a highly electrically conductive methyl cellulose-silver nanoparticles-polyaniline (MC-AgNPs-PANi) nanocomposite. For this purpose, silver nitrate was used as a precursor for the preparation of AgNPs. Glycerol was added to

the reaction medium to increase the ductility of the resulting films, at the same time it acts as a co-reducing agent.

Methyl cellulose is used for the first time in producing MC-AgNPs-PANi nanocomposite. In addition to its function as both reducing the silver ions to AgNPs and capping agent for the produced AgNPs, MC is a film forming polymer that is responsible for producing the conductive film of the MC-AgNPs-PANi nanocomposite.

The Formation of AgNPs is expressed as the absorbance of the colloidal solution of MC-AgNPs-PANi nanocomposite after the end of the synthesis reaction. AgNPs so obtained are characterized and confirmed by FTIR. The crystallinity profile is obtained by XRD. The thermal behavior is performed by TGA. The morphology and particle size are measured by TEM.

Conductive glass, conductive film, and conductive fabrics, namely, cotton, polyester and non-woven are prepared and tested for their conductivity by measuring the resistivity of the film or the fabric.

## Experimental

### Materials

Methyl cellulose, aniline, glycerol and silver nitrate were of laboratory grade and used as received without further purification.

Cotton, polyester and non-woven fabrics were purchased from local market and used as it is without further modification.

### Method

#### Synthesis of MC-AgNPs-PANi nanocomposite

A 100 ml of 1% (w/v) MC solution is placed in a 150 ml sealable glass bottle with small magnetic bar and then placed in a water bath heated by a thermostatic hot plate with a magnetic stirrer. A 1% (v/v) of aniline is added and well stirred until completely mixed with MC. After mixing, a 1% (v/v) glycerol is added and the glass bottle is sealed and left under stirring for five minutes until complete homogenization. It is worth to mention that glycerol acts as a co-surfactant to equilibrate the hydrophilic (aqueous silver nitrate) and hydrophobic (aniline) proximities [60]. After that, a 1 ml of 1M silver nitrate is added to obtain silver nitrate with concentration of 0.17% (w/v) and well stirred. The whole components are left under stirring at 90°C for 1 h after which the

reaction vessel is removed from the water bath and allowed to cool.

#### *Conductive Film Forming*

MC-AgNPs-PANi nanocomposite film is prepared by pouring a certain volume of the nanocomposite in a petry dish and allowed to dry at 100°C. After drying the film is peeled and kept in a sealable plastic bag for use in characterization.

#### *Conductive Fabrics Forming*

Conductive cotton, polyester, and non-woven fabrics are obtained by placing a 3cm<sup>3</sup> piece of fabric in a square vessel with the same fabric area and coating the surface of the fabric by pouring a certain volume of MC-AgNPs-PANi nanocomposite solution over the fabric area and allowed to dry at 100°C. After drying the fabrics were removed and kept in a sealable plastic bag for use in characterization.

#### *Characterizations and analyses*

Camspec M 105 Spectrophotometer, Spectronic Camspec Ltd, UK was used to measure the absorbance of AgNPs in the colloidal solution of MC-AgNPs-PANi nanocomposite. The spectra of AgNPs were recorded at wavelength range from 300 to 600 nm.  $\lambda_{max}$  at 390-440 is characteristic to AgNPs. Synthesis of AgNPs is expressed as absorbance of the colloidal solution of the nanocomposite. The absorbance, the broadening and the wavelength of the band measure the intensity of AgNPs in the colloidal solution. False readings were recorded for the first measured samples a result of the high concentration of the AgNPs, so and to avoid these false readings, all samples were diluted "200" times of the original sample using distilled water.

FTIR spectra of MC-AgNPs-PANi nanocomposite film was performed using Jasco FTIR-4700 with ATR Pro One, Japan. The data were recorded from 400 to 4000 cm<sup>-1</sup>.

Thermogravimetric analysis (TGA) of MC-AgNPs-PANi nanocomposite film was obtained using SDT Q600 V20.9 Build 20, Universal V4.5A TA Instruments. To do so, an accurate weight of the above-mentioned sample was heated from 0°C to 600°C using a heating rate of 5°C/min in a nitrogen atmosphere. Weight of the sample was 2.124 mg. The DSC data is obtained from software analysis of TGA measurement. All discussions depend on TGA measurements.

X-ray diffraction (XRD) pattern of AgNPs film was obtained using Empyrean, pxccl3D,

Amedipixz collaboration, PANALYTICAL, Netherlands with Cu-K- radiation ( $\lambda = 0.15406$  nm) in the 2 $\theta$  range from 10° to 80° and 30 mA, 45 kV.

Transmission electron micrographs (TEM), and selected area electron diffraction (SAED) for the colloidal solution of MC-PANi-AgNPs nanocomposite were measured by means of a JEOLJEM- 1200 Transmission Electron Microscope (TEM). The samples were prepared by placing a drop of the colloidal solution on a 400-mesh copper grid coated by an amorphous carbon film and evaporating the solvent in air at room temperature. The average diameter of the silver nanoparticles was determined from the diameter of nanoparticles found in several chosen areas in enlarged microphotographs.

Scanning electron micrographs (SEM) and energy dispersive X-ray spectroscopy (EDAX) spectrum of selected area of MC-AgNPs-PANi nanocomposite film were carried out using Quanta FEG 250 equipped with energy dispersive spectrophotometer to follow both the elemental change in surface morphology as well as to verify the elemental composition of the MC-AgNPs- PANi nanocomposite film.

Conductivity of the nanocomposite film, the nanocomposite coated glass or the nanocomposite coated fabrics was measured by calculating the mean value of measuring the resistivity ( $M\Omega$ ) by a resistivity meter at five different areas (1 cm<sup>2</sup>) of film, glass or fabric. The conductivity is the reciprocal of resistivity.

1 megohm [ $M\Omega$ ] = 1000000 reciprocal siemens [1/S]

## **Results and Discussions**

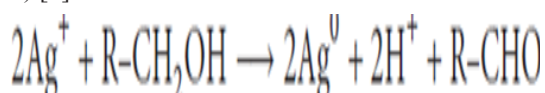
### *Synthesis and reproducibility of silver nanoparticles*

Figure 1 shows the absorbance of the colloidal solution at wavelength range from 320-600 nm for five different samples of AgNPs prepared at the same reaction conditions. At the beginning of the synthesis reaction the color of the solution was white which turned dark brown by the end of the reaction (Figure 1a). The solution had to be diluted by 1: 200 due to the high intensity of the AgNPs which could be predicted from the intensity of the color of the colloidal solution. It is known that concentrated solutions deviate from Beer Lambert's law and give false results. The dark brown color of the concentrated solutions

of silver nanoparticles becomes yellow after dilution (Figure 1 b). The intensity of the color changes depending on the concentration of the nanoparticles. The figure shows the formation of AgNPs where a bell-like curve with a peak appears at about 440 nm is obtained [61, 62].

The figure also confirms the change in the color of the reaction mixture from white at the beginning of the reaction to a dark brown color due to the formation of AgNPs.

The conversion of silver ions  $\text{Ag}^+$  to nano silver  $\text{Ag}^0$  is due to several reducing agents present in the reaction medium, namely: MC, and glycerol as bearing OH groups on their structure. The so-called "alcohol reduction process" is a very general process to produce metal nanoparticles, often stabilized by organic polymers. In general, the alcohols which were useful reducing agents contained  $\alpha$ -hydrogen and were oxidized to the corresponding carbonyl compounds. The oxidation of primary alcohols ( $\text{R}-\text{CH}_2\text{OH}$ ) by  $\text{Ag}^+$  is also well established; the reaction is slow and requires heating to be accelerated: (equation 2) [6].



**Equation 2: Oxidation/reduction of the OH/ $\text{Ag}^+$  and formation of  $\text{Ag}^0$**

Silver ions also oxidizes aniline to PANi and in its turn they are reduced to AgNPs. expressed as the absorbance of AgNPs of the colloidal solution. Figure 1 shows the absorbance results of the five experiments. The figure shows the appearance of the bell shape for all samples, confirming the formation of silver nanoparticles and the approximation of the absorbance values of the five samples, which indicates the reproducibility and stability of the synthesis process.

*Characterization of MC-PANi-AgNPs nanocomposite*

*FTIR*

To confirm the formation of PANi and AgNPs in the nanocomposite, FTIR spectra was carried out.

FTIR was performed from 400-4000  $\text{cm}^{-1}$ . In Figure 2, the spectra of the nanocomposite film is displayed. A film consisting of pure MC is used as reference sample whose absorption peaks can be assigned to peaks known from literature [63]. This includes, among others, the bands for the

O–H stretching vibration at around 3444  $\text{cm}^{-1}$  and the C–H stretching vibration approximately 2903  $\text{cm}^{-1}$ . The FTIR spectrum shows the most characteristic bands of the nanocomposite film. Among these bands, the band at about 3440  $\text{cm}^{-1}$  characteristic for OH stretching of MC and glycerol and NH stretching of PANi. The CH stretching band at about 2865  $\text{cm}^{-1}$ . The band at 2790  $\text{cm}^{-1}$  is characteristic for CH stretching of the methyl group. The band at about 1535  $\text{cm}^{-1}$  characteristic for benzene ring vibrations. The three bands at about 1360, 1287 and 1226  $\text{cm}^{-1}$  are characteristic for CN aromatic stretching. The band at about 1050  $\text{cm}^{-1}$  is characteristic for the CN stretching. Finally the band at about 905  $\text{cm}^{-1}$  is characteristic for CN aromatic bending. These bands confirm the formation of PANi [27, 36].

*TGA*

Thermal analysis has been performed for MC-PANi-AgNPs nanocomposite film using the TGA and DSC techniques as described in the "Methods" section.

Results obtained from the TGA curve (Figure 3) showed an initial weight loss of 10.01% of the original weight took place at up to 350°C. This weight loss is characterized by slow rate. The increase in the percent of weight loss and the temperature at which the loss took place at this stage is mainly due to the moisture content, bound water, volatile components and oligomers. This weight loss could be due to the high moisture content as a result of the hydrophilicity of MC chain. It could also be due to the decomposition of short chains (lower molar mass) of MC. These short chains possibly formed due to: 1) the acid degradation that could take place during the synthesis reaction as a result of the formation of nitric acid as a byproduct (equation 1) and 2) the oxidative degradation that may take place due to oxidation of the OH (equation 2). Both acid degradation and oxidative degradation would be favored by the high temperature (90°C) at which the synthesis took place [64]. A main stage of decomposition represents a weight loss of 65.84% of the original weight started at about 350°C and ended at about 525°C. This stage is involved in the decomposition of the MC-PANi-AgNPs nanocomposite and is characterized by a fast rate of decomposition. The high temperature (525°C) at which the main stage of decomposition took place reflects the thermal stability of the produced MC-PANi-AgNPs film [36].

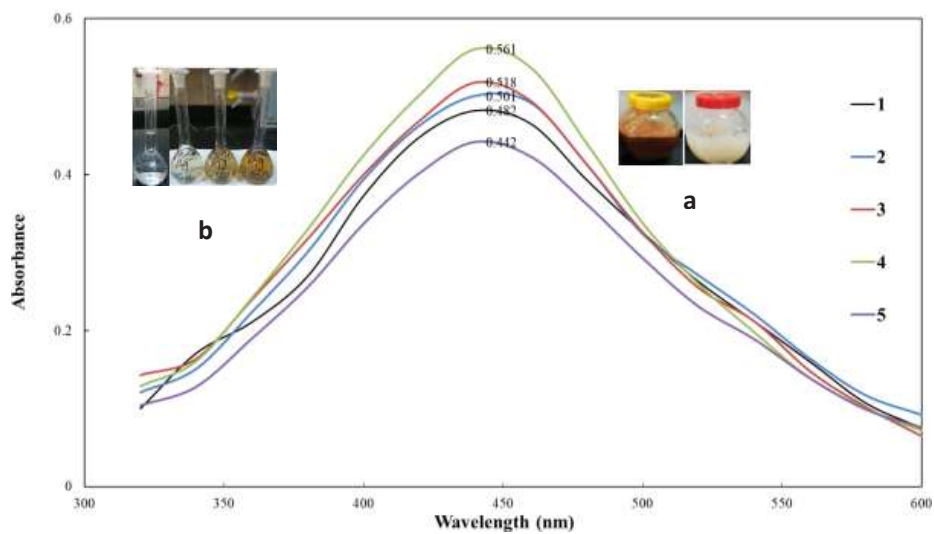


**Fig. 1: Synthesis and reproducibility of silver nanoparticles**

MC, (1% w/v); AgNO<sub>3</sub>, (0.17% w/v); Aniline, (1% v/v); Glycerol, (1% v/v); Temp. 90oC; Time, 1h.

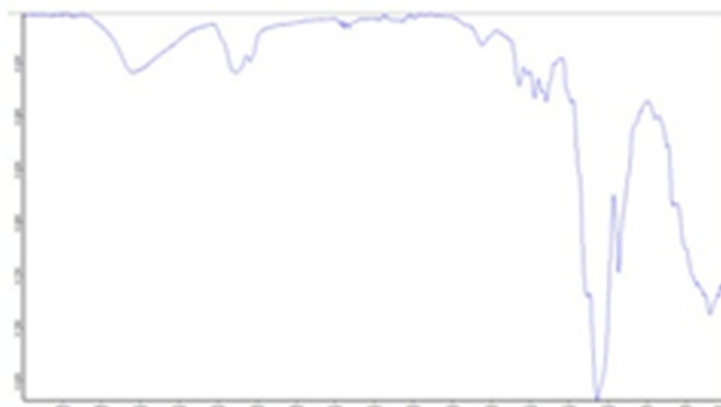


**Fig. 2: FTIR of MC-PANi-AgNPs nanocomposite film**

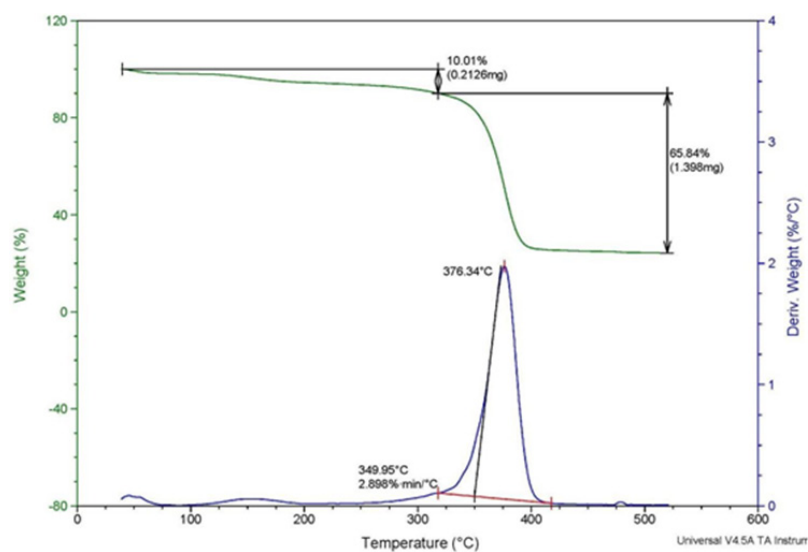


**Fig. 3: TGA of MC-PANi-AgNPs nanocomposite film**

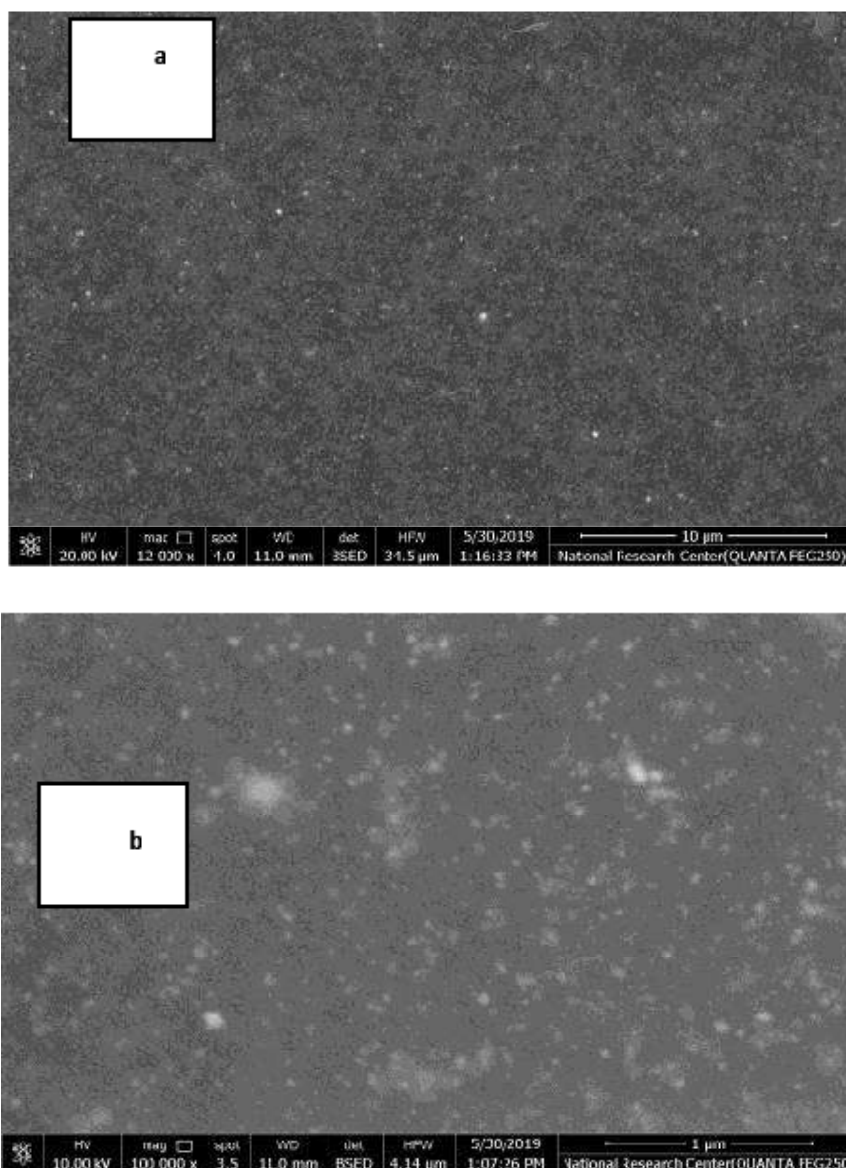
*Scanning electron micrograph (SEM) and EDAX*

Figure 4 (a, b, c) shows the SEM of MC-PANi-AgNPs film at two different magnifications, namely: a) 12000 and b) 100000 and EDAX (c).

It could be noticed from the micrographs (a) and (b) the well distributed round shiny silver particles over the whole area under investigation.

Figure 4 (c) shows the EDAX and report of the percentages of C, O, Ag and N elements in

a chosen area of the SEM of MC-PANi-AgNPs nanocomposite film. As seen, The percentage of carbone, oxygen, silver and nitrogen elements are 50.95%, 39.78, 8.35 and 0.92 of the nanocomposite respectively. Carbon element refers to the carbon in both MC and PANi, oxygen refers to oxygen of the hydroxyl groups of MC and glycerol, Ag to the AgNPs and nitrogen to the PANi. AgNPs represents a good percentage of the nonocomposite as many parameters participated in the reduction process, namely, aniline, glycerol and MC.



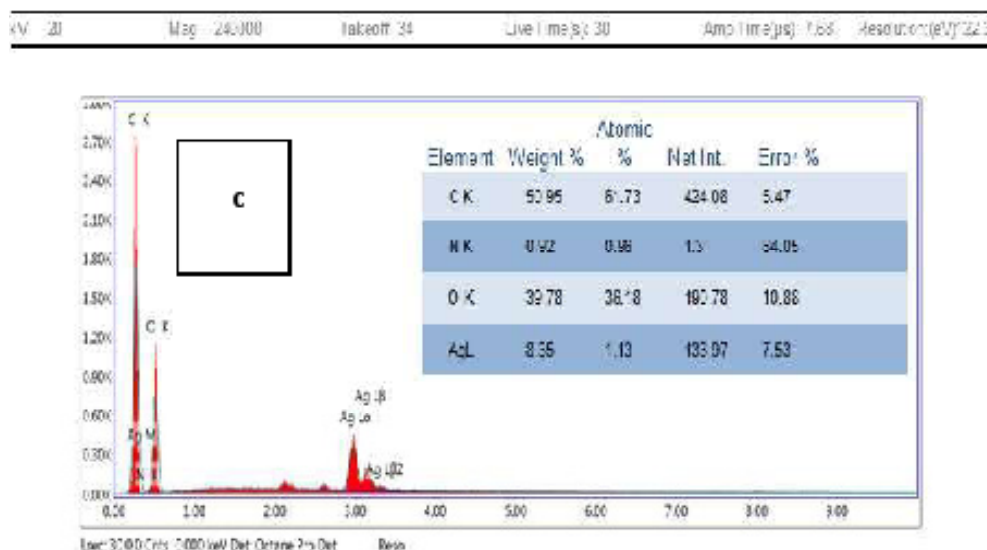


Fig. 4 (a-c): SEM and EDAX of MC-PANi-AgNPs nanocomposite film

#### TEM and SEAD

Figure 5 (a, b) shows TEM micrographs and Particle size distribution histogram for PANi-AgNPs nanocomposite solution.

In Figure 5 (a), it could be seen that AgNPs exhibits different particle shapes. The average diameter of AgNPs was determined from the diameter of nanoparticles found in several chosen areas in enlarged microphotograph of Figure 5 (a). Consequently, Figure 5 (b) shows the particle size distribution of AgNPs. Particles size ranged from 4-36 nm, highest and lowest particles size count were 10-15 and 30-36 nm respectively.

Figure 5 (c-g) shows SAED of the colloidal solution of MC-PANi-AgNPs nanocomposite.

Figure 5 (c) shows enlarged TEM of AgNPs at which the different shapes of the nanoparticles are very clear. Whereas, Figure 5 (d) shows more enlarged TEM at which d-spacing of the particles is clearly presented in the micrograph. The size of these particles ranged from 12-27 nm.

In addition, the magnified image in Figure 5 (e and f) shows a d-spacing value of 0.22 nm corresponding to the (111) plane (JCPDS file no. 04-0783).

Finally, SAED pattern of AgNPs exhibits ring pattern with bright spots ((Figure 5 “g”) displaying polycrystallinity corresponding to the (002), (111), (200), (220), (311), (222) and (420) planes matching to the FCC structure of AgNPs (JCPDS file no. 04-0783).

#### XRD

Figure 6 shows the XRD pattern of MC-PANi-AgNPs nanocomposite film synthesized by in-situ oxidative polymerization of aniline to PANi by AgNO<sub>3</sub> and the reduction of the silver nitrate to AgNPs by aniline, glycerol and MC. The sharp peaks at 2 $\theta$  values = 24.6 $^\circ$ , 38.67 $^\circ$ , 44.91 $^\circ$ , 64.62 $^\circ$  and 77.20 $^\circ$  can be assigned to the face centered cubic (FCC) phase of silver (002), (111), (200), (220) and (311), respectively [65] which is in agreement with the data found in the literature [66-69]. The existence of sharp peaks clearly indicates the presence of AgNPs in the composites with their crystalline nature. The broad peak at 2 $\theta$  value = 10–20 $^\circ$  could be due to amorphous regions in MC with two weak peaks at 8, 12 could be due to the crystalline regions in MC [70].

TEM image (Figure 5 “f”) showed d-spacing of 0.22 nm corresponding to the (111) plane. Similarly, the intense XRD peak at 2 $\theta$  value = 38.67 $^\circ$  (Figure 6) is corresponding to the intense reflection from (111) plane matching to the FCC structure of AgNPs. These results agreements from both TEM and XRD assure the crystalline structure of AgNPs in the MC-PANi-AgNPs nanocomposite.

#### Conductivity of MC-PANi-AgNPs nanocomposite

MC-PANi-AgNPs nanocomposite was utilized to impart conductivity properties for glass, film, cotton fabric, polyester fabric and non-woven fabric. Table 1 show the resistivity and conductivity of the tested samples.

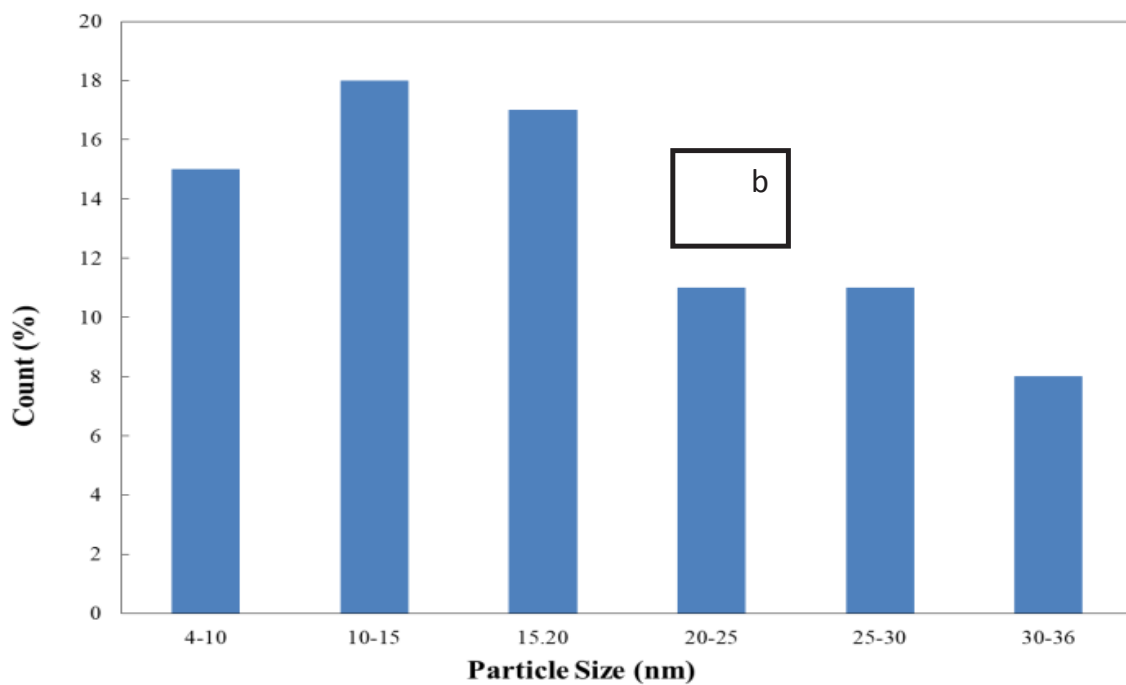
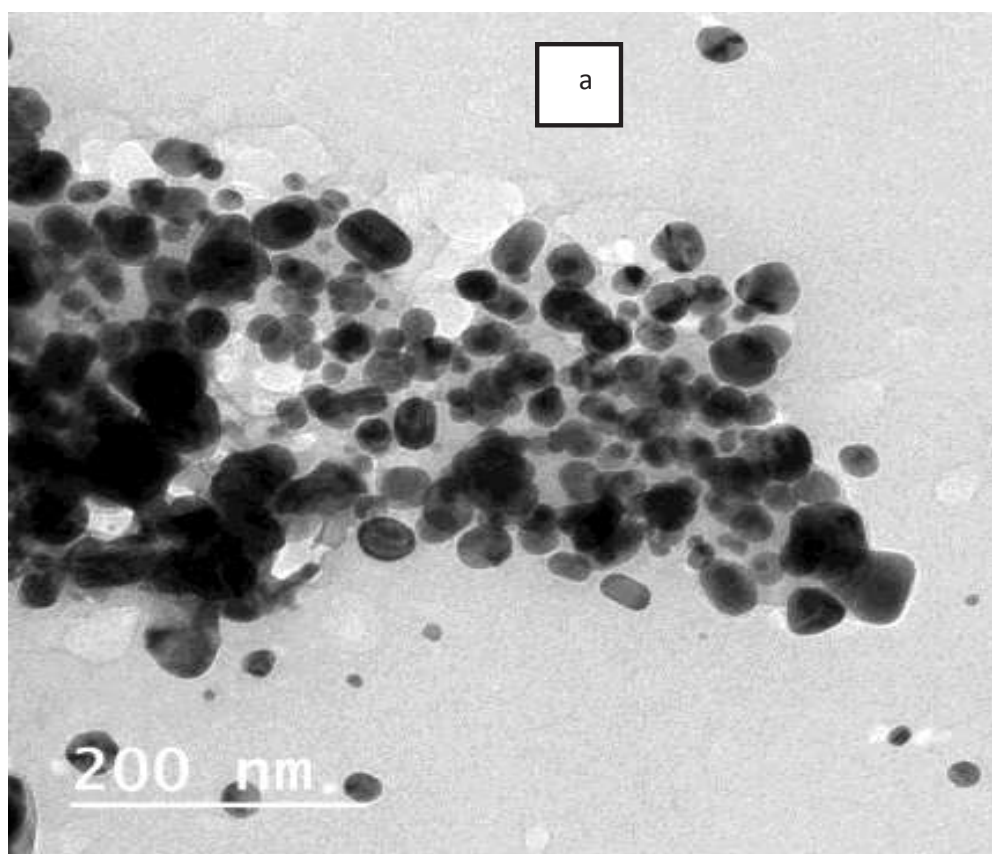
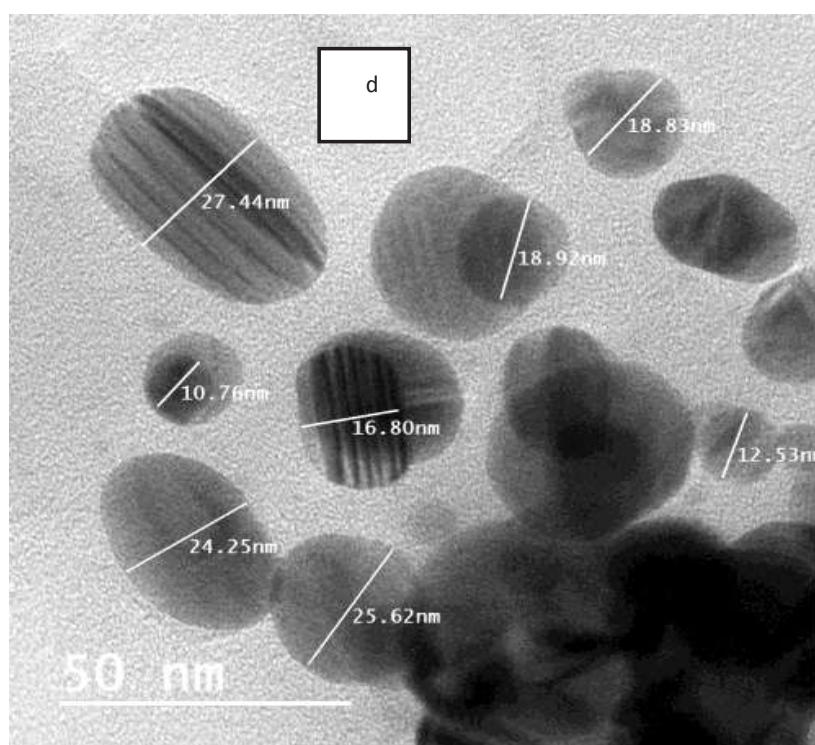
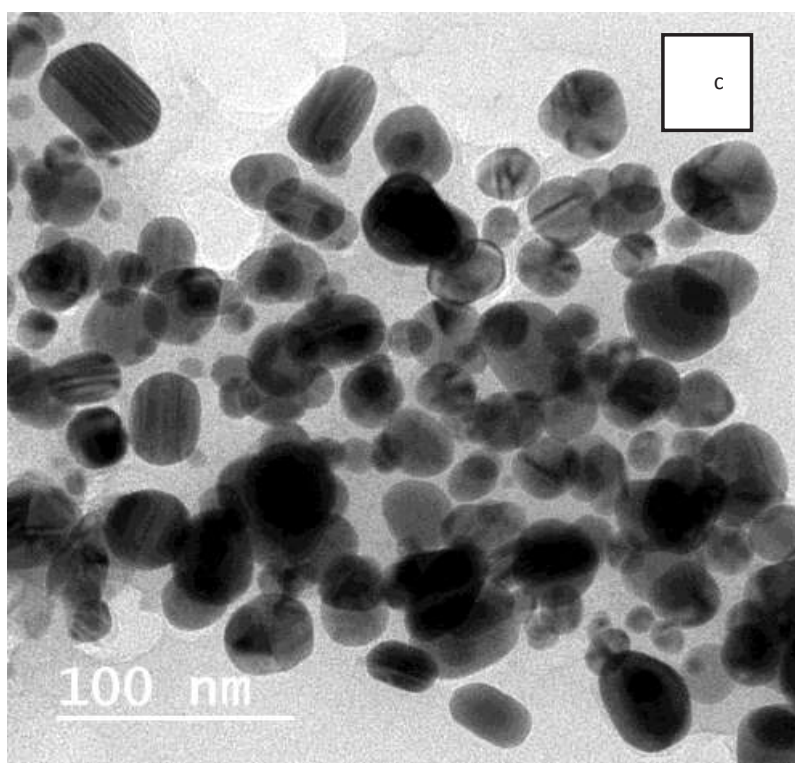
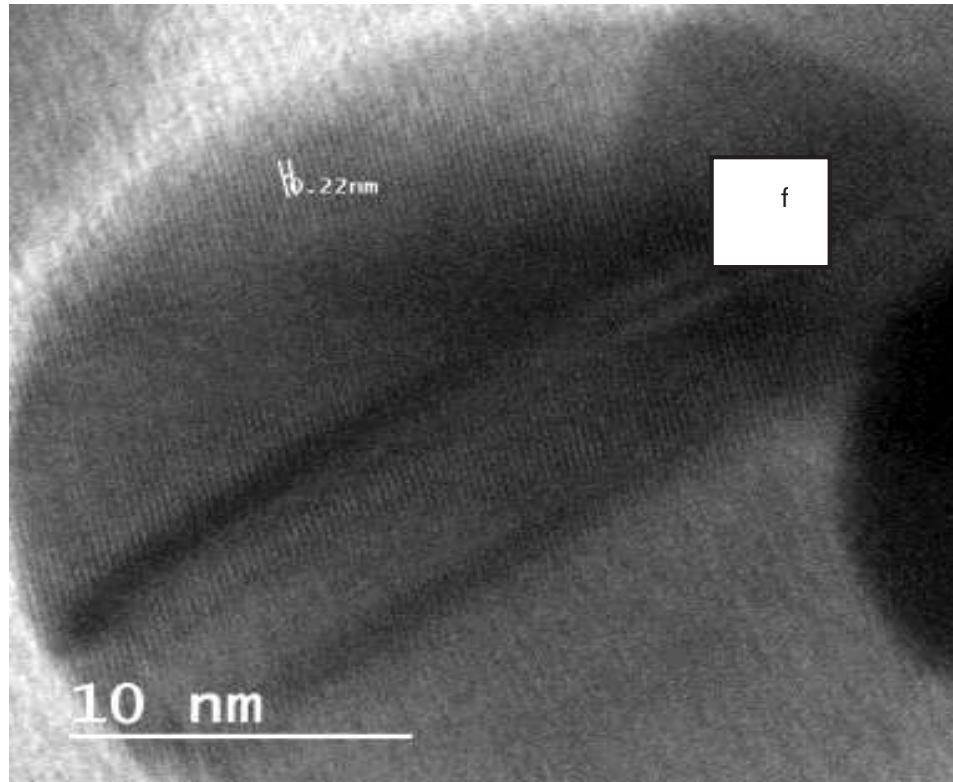
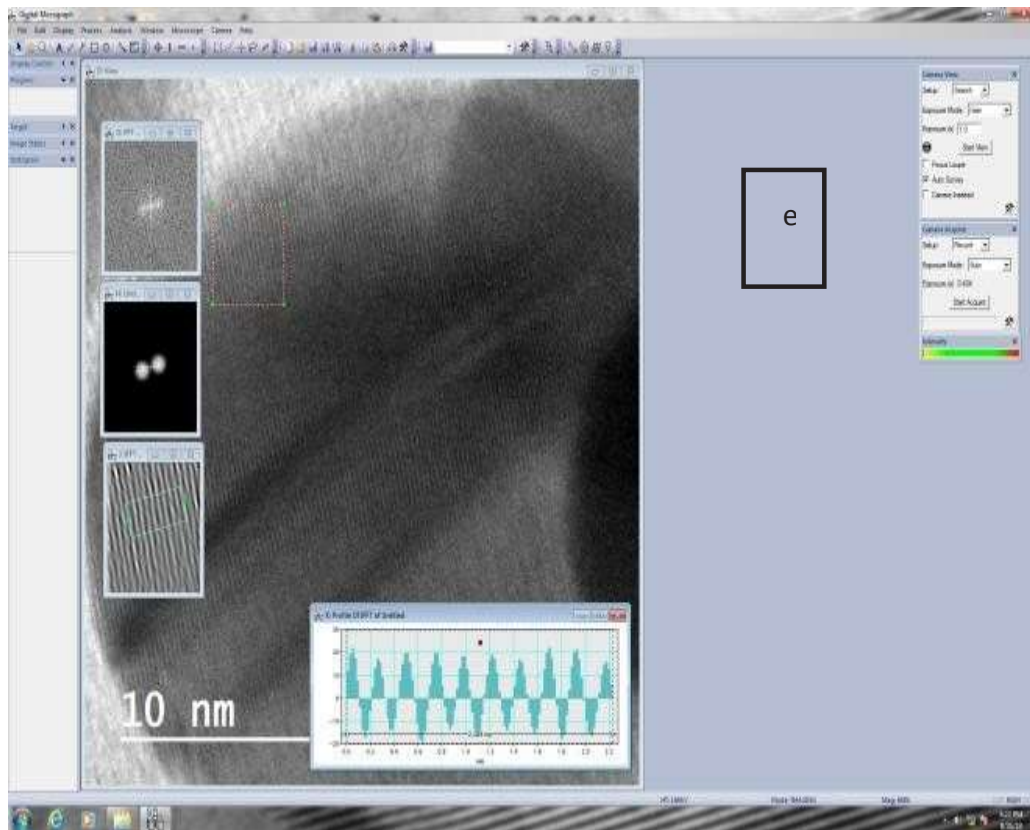


Fig. 5 (a, b): TEM and particle size distribution of MC-PANi-AgNPs nanocomposite





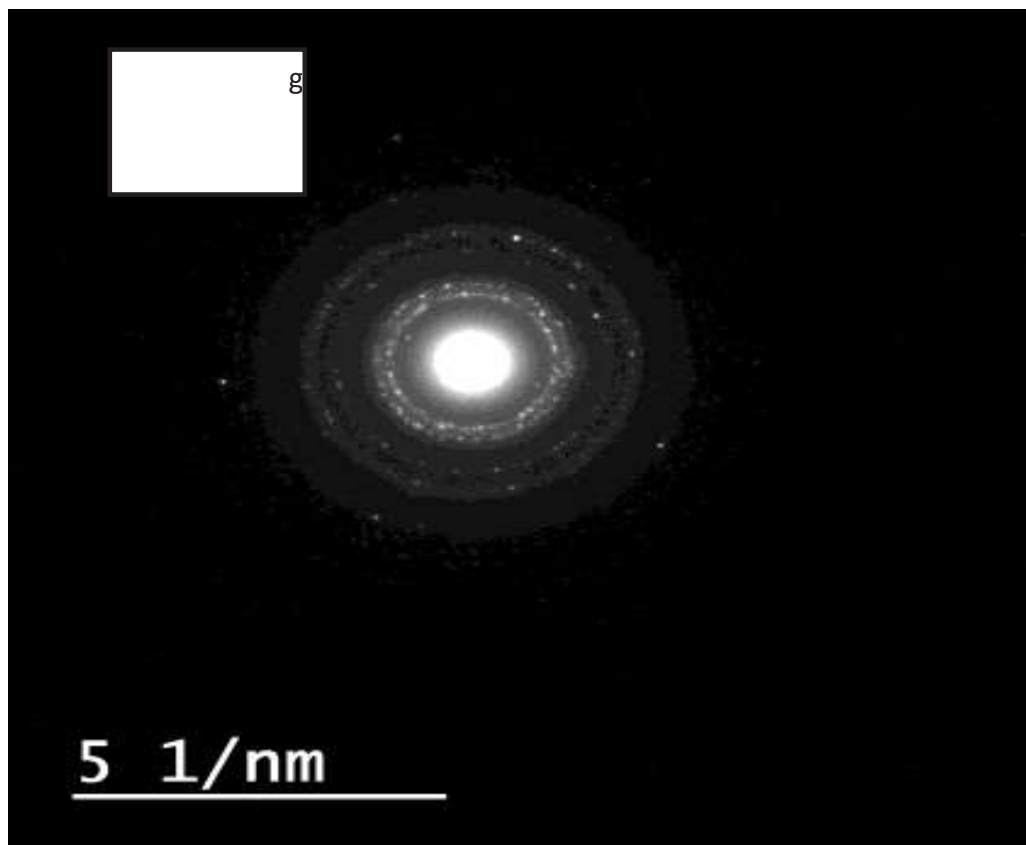


Fig. 5 (c-g): SAED of the colloidal solution of MC-PANi-AgNPs nanocomposite

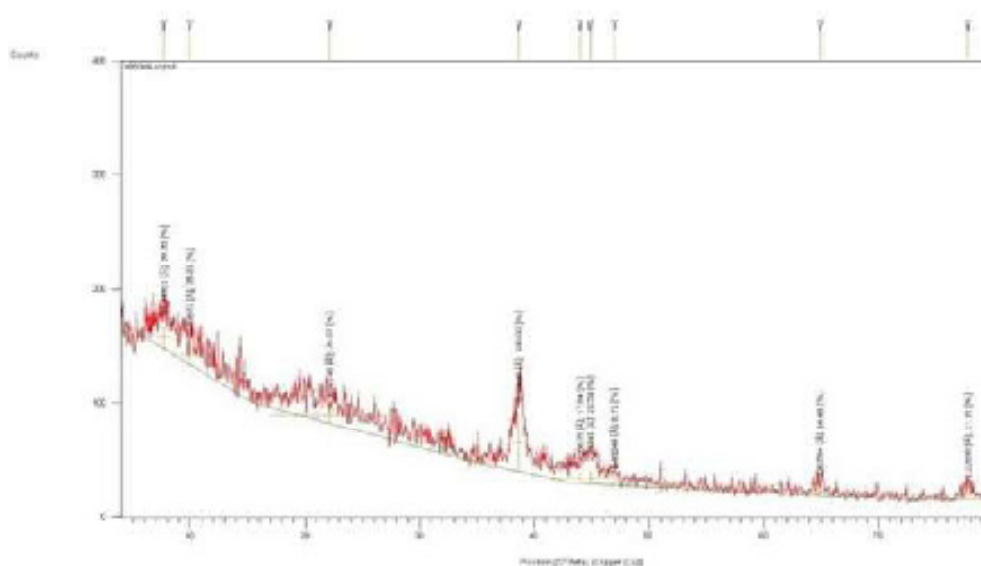


Fig. 6: XRD of MC-PANi-AgNPs nanocomposite film

It can be seen from Table 1 that all samples showed good conductivity values; thus it could be assumed semi-conductors. The variation in the conductivity values (S) depends on the type of the sample and follows the descending order:

Glass = Film > Polyester > Non- Woven > Cotton

This order could be attributed to the electrical charge on the fabric surface as well as its ability to retain the nanocomposite within its structure.

Sample	Resistivity, megaohm (MΩ)	Resistivity, ohms (Ω)	Conductivity, Siemens (S)
Glass	1	1000000	1E-06
Film	1	1000000	1E-06
Cotton	18	18000000	5.56E-08
Polyester	8	8000000	1.25E-07
Non-Woven	10	10000000	1E-07

### Conclusions

A novel method for synthesis of MC-PANi-AgNPs nanocomposite was developed. AgNPs formed was evaluated by measuring the absorbance of the colloidal solution of the nanocomposite using vis-spectrophotometer. Reaction conditions for the preparation of MC-PANi-AgNPs nanocomposite were: The nanocomposite was: MC, (1% w/v); AgNO<sub>3</sub>, (0.17% w/v); Aniline, (1% v/v); Glycerol, (1% v/v); Temp. 90°C; Time, 1h. Reproducibility of the nanocomposite at the same reaction conditions revealed that the synthesis process is consistent and the absorbance of five samples were nearly the same. FTIR analysis showed NH stretching at 3440 cm<sup>-1</sup>, benzene ring vibrations at 1535 cm<sup>-1</sup>, CN aromatic stretching at 1360, 1287 and 1226 cm<sup>-1</sup>, and CN aromatic bending at 905 cm<sup>-1</sup> which confirms the formation of PANi. SEM showed a well distributed round AgNPs. EDAX of selected area of SEM showed that the percentage of carbone, oxygen, silver and nitrogen elements are 50.95%, 39.78, 8.35 and 0.92 of the nanocomposite respectively. XRD pattern showed poly crystallinity proved by the sharp peaks at 2θ values = 24.6°, 38.67°, 44.91°, 64.62° and 77.20° which can be assigned to the FCC phase of silver (002), (111), (200), (220) and (311), respectively. TEM and particle size distribution showed AgNPs with different particle shapes. The average diameter of AgNPs ranged from 4-36 nm, highest and lowest particles size count were 10-15

and 30-36 nm respectively. Magnified TEM image showed a d- spacing of 0.22 nm corresponding to Ag (111) plane which is in agreement with the intense peak of XRD at 2θ value = 38.67°. SAED pattern of AgNPs exhibits ring pattern with bright spots displaying polycrystallinity corresponding to the (002), (111), (200), (220), (311), (222) and (420) planes matching to the FCC structure of Ag. Conductivity measurements showed that samples treated with the nanocomposite showed good conductivity (S) and could be assumed semi-conductors. The conductive samples follow the descending order:

Glass = Film > Polyester > Non- Woven > Cotton

### Acknowledgement

The authors Acknowledge the Faculty of Science and Arts in Qurayyate, Jouf University, Saudi Arabia for facilities provided to prepare and analyze the materials of the current work.

### References

- Konvičková, Z., Holišová, V., Kolenčík, M., Niide, T., et al., Phytosynthesis of colloidal Ag-AgCl nanoparticles mediated by *Tilia* sp. leachate, evaluation of their behaviour in liquid phase and catalytic properties. *Colloid. Polym. Sci.* 2018, 296, 677–687.
- El-Naggar, M. E.-S., in: El-Naggar, M. E.-S. (Ed.), *Scholars' Press, Germany* 2015, p. 388.
- El-Sheikh, M. A., A novel photo-grafting of acrylamide onto carboxymethyl starch. 1. Utilization of CMS-g-PAAm in easy care finishing of cotton fabrics. *Carbohydr. Polym.* 2016, 152, 105-118.
- El-Sheikh, M. A., *NSTI: Advanced Materials - TechConnect Briefs 2015* 2015, pp. 55-59.
- El-Sheikh, M. A., Ibrahim, H. M., One Step Photopolymerization of N, N-Methylene Diacrylamide and Photocuring of Carboxymethyl Starch-Silver Nanoparticles onto Cotton Fabrics for Durable Antibacterial Finishing. *International Journal of Carbohydrate Chemistry* 2014, 2014, 1-9.
- El-Sheikh, M. A., A Novel Photosynthesis of Carboxymethyl Starch-Stabilized Silver Nanoparticles. *The Scientific World Journal* 2014, 2014, 1-11.
- El-Sheikh, M. A., El-Rafie, S. M., Abdel-

- Halim, E. S., El-Rafie, M. H., Green Synthesis of Hydroxyethyl Cellulose-Stabilized Silver Nanoparticles. *Journal of Polymers* 2013, 2013, 1-11.
8. El-Sheikh, M. A., El-Gabry, L. K., Ibrahim, H. M., Photosynthesis of Carboxymethyl Starch-Stabilized Silver Nanoparticles and Utilization to Impart Antibacterial Finishing for Wool and Acrylic Fabrics. *Journal of Polymers* 2013, 2013, 1-9.
  9. El-Sheikh, M. A., 7th Aachen-Dresden International Textile Conference, DWI an der RWTH Aachen e.V., Aachen, Germany 2013, pp. 1-43.
  10. Hebbalalu, D., Lalley, J., Nadagouda, M. N., Varma, R. S., Greener Techniques for the Synthesis of Silver Nanoparticles Using Plant Extracts, Enzymes, Bacteria, Biodegradable Polymers, and Microwaves. *ACS Sustainable Chemistry & Engineering* 2013, 1, 703–712.
  11. Hebeish, El-Rafie, M. H., El-Sheikh, M. A., Seleem, A. A., El-Naggar, M. E., Antimicrobial Wound Dressing and Anti-inflammatory Efficacy of Silver Nanoparticles. *Int. J. Biol. Macromol.* 2014, 65 509–515.
  12. Hebeish, A., El-Rafie, M. H., El-Sheikh, M. A., El-Naggar, M. E., Nanostructural Features of Silver Nanoparticles Powder Synthesized through Concurrent Formation of the Nanosized Particles of Both Starch and Silver. *Journal of Nanotechnology* 2013, 2013, 1-10.
  13. Hebeish, A., Shaheen, T. I., El-Naggar, M. E., Solid state synthesis of starch-capped silver nanoparticles. *Int. J. Biol. Macromol.* 2016, 87, 70-76.
  14. Huang, Y., Li, J., Yin, T., Jia, J., et al., A novel all-solid-state ammonium electrode with polyaniline and copolymer of aniline/2,5-dimethoxyaniline as transducers. *J. Electroanal. Chem.* 2015, 741, 87-92.
  15. Malathi, S., Ezhilarasu, T., Abiraman, T., Balasubramanian, S., One pot green synthesis of Ag, Au and Au-Ag alloy nanoparticles using isonicotinic acid hydrazide and starch. *Carbohydr. Polym.* 2014, 111, 734-743.
  16. Mandal, A., Sekar, S., Seeni Meera, K. M., Mukherjee, A., et al., Fabrication of collagen scaffolds impregnated with sago starch capped silver nanoparticles suitable for biomedical applications and their physicochemical studies. *Phys. Chem. Chem. Phys.* 2014, 16, 20175-20183.
  17. Raveendran, P., Fu, J., Wallen, S. L., Completely "green" synthesis and stabilization of metal nanoparticles. *J. Am. Chem. Soc.* 2003, 125, 13940-13941.
  18. Hebeish, A., El-Rafie, M. H., El-Sheikh, M. A., El-Naggar, M. E., Ultra-Fine Characteristics of Starch Nanoparticles Prepared Using Native Starch With and Without Surfactant. *Journal of Inorganic and Organometallic Polymers and Materials* 2014, 24, 515–524.
  19. Hebeish, A. A., Ramadan, M. A., Montaser, A. S., Farag, A. M., Preparation, characterization and antibacterial activity of chitosan-g-poly acrylonitrile/silver nanocomposite. *Int. J. Biol. Macromol.* 2014, 68, 178-184.
  20. Abdelgawad, A. M., Hudson, S. M., Rojas, O. J., Antimicrobial wound dressing nanofiber mats from multicomponent (chitosan/silver-NPs/polyvinyl alcohol) systems. *Carbohydr. Polym.* 2014, 100, 166-178.
  21. Tsai, T. T., Huang, T. H., Chang, C. J., Yi-Ju Ho, N., et al., Antibacterial cellulose paper made with silver-coated gold nanoparticles. *Sci. Rep.* 2017, 7, 3155.
  22. Wan, C., Li, J., Cellulose aerogels functionalized with polypyrrole and silver nanoparticles: In-situ synthesis, characterization and antibacterial activity. *Carbohydr. Polym.* 2016, 146, 362-367.
  23. Yan, J., Abdelgawad, A. M., El-Naggar, M. E., Rojas, O. J., Antibacterial activity of silver nanoparticles synthesized In-situ by solution spraying onto cellulose. *Carbohydr. Polym.* 2016, 147, 500-508.
  24. Jayasudha, S., Priya, L., Vasudevan, K. T., Preparation and characterization of polyaniline/Ag nanocomposites. *International Journal of ChemTech Research* 2014, 6, 1821-1823.
  25. Kan, Y., An All-Solid-State Ammonium Ion-Selective Electrode Based on Polyaniline as Transducer and Poly (o-phenylenediamine) as Sensitive Membrane. *International Journal*

- of Electrochemical Science 2016, 9928-9940.
26. Ali, N. A., Hassan, S. M., Huseen, S. I., Structural, thermal and electrical properties of prepared polyaniline / silver nanocomposites. *International Journal of Applied Engineering Research* 2017, 12, 14869-14873.
  27. Bober, P., Stejskal, J., Trchová, M., Prokeš, J., Sapurina, I., Oxidation of Aniline with Silver Nitrate Accelerated by p-Phenylenediamine: A New Route to Conducting Composites. *Macromolecules* 2010, 43, 10406-10413.
  28. Jing, S., Xing, S., Yu, L., Wu, Y., Zhao, C., Synthesis and characterization of Ag/polyaniline core-shell nanocomposites based on silver nanoparticles colloid. *Mater. Lett.* 2007, 61, 2794-2797.
  29. Farrage, N. M., Oraby, A. H., Abdelrazek, E. M. M., Atta, D., Synthesis, characterization of Ag@PANI core-shell nanostructures using solid state polymerization method. *Biointerface Research in Applied Chemistry* 2019, 9, 3934-3941.
  30. Khan, M., Husain, Q., Safeguarding the catalytic activity and stability of polyaniline chitosan silver nanocomposite bound beta-galactosidase against product inhibitors and structurally related compound. *Artificial Cells, Nanomedicine and Biotechnology* 2019, 47, 1075-1084.
  31. Li, Z., Li, J., Lin, W., Preparation and characterization of Ag/polyaniline nanocomposite. *Zhongnan Daxue Xuebao (Ziran Kexue Ban)/Journal of Central South University (Science and Technology)* 2014, 45, 1784-1789.
  32. Li, Z., Hua, S., Lu, J., Conductivity of silver/polyaniline core-shell nanocomposite. *Gaofenzi Cailiao Kexue Yu Gongcheng/Polymeric Materials Science and Engineering* 2013, 29, 46-49.
  33. Li, Z. H., Li, Z., Lin, W., Effect of different doping acids on the structure and conductivity of silver/polyaniline nanocomposites. *Acta Polymerica Sinica* 2013, 827-831.
  34. Wang, Q., Zhou, Y., Zhou, J., Wu, R., et al., Doped PANI Coated Nano-Ag Electrode for Rapid In-Situ Detection of Bromide in Seawater. *Coatings* 2019, 9, 1-14.
  35. Abd El-Ghaffar, M. A., Shaffei, K. A., Fouad Zikry, A. A., Mohamed, M. B., Marzouq, K. A. G., Novel conductive nano-composite ink based on poly aniline, silver nanoparticles and nitrocellulose. *Egypt. J. Chem.* 2016, 59, 429-443.
  36. Pashaei, S., Hosseinzadeh, S., Hosseinzadeh, H., TGA investigation and morphological properties study of nanocrystalline cellulose/ag-nanoparticles nanocomposites for catalytic control of oxidative polymerization of aniline. *Polym. Compos.* 2019, 40, E753-E764.
  37. Poyraz, S., Cerkez, I., Huang, T. S., Liu, Z., et al., One-step synthesis and characterization of polyaniline nanofiber/silver nanoparticle composite networks as antibacterial agents. *ACS Applied Materials and Interfaces* 2014, 6, 20025-20034.
  38. Sultana, S., Ahmad, N., Faisal, S. M., Owais, M., Sabir, S., Synthesis, characterisation and potential applications of polyaniline/chitosan-Ag-nano-biocomposite. *IET Nanobiotechnology* 2017, 11, 835-842.
  39. Johnston, J. H., Moraes, J., Borrmann, T., Conducting polymers on paper fibres. *Synth. Met.* 2005, 153, 65-68.
  40. Hou, W., Xiao, Y., Han, G., Lin, J. Y., The applications of polymers in solar cells: A review. *Polymers* 2019, 11.
  41. Li, C., Zhang, L., Ding, L., Ren, H., Cui, H., Effect of conductive polymers coated anode on the performance of microbial fuel cells (MFCs) and its biodiversity analysis. *Biosens. Bioelectron.* 2011, 26, 4169-4176.
  42. Kanungo, M., Kumar, A., Contractor, A. Q., Studies on electropolymerization of aniline in the presence of sodium dodecyl sulfate and its application in sensing urea. *J. Electroanal. Chem.* 2002, 528, 46-56.
  43. Li, Z. F., Ruckenstein, E., Strong adhesion and smooth conductive surface via graft polymerization of aniline on a modified glass fiber surface. *J. Colloid Interface Sci.* 2002, 251, 343-349.
  44. Yin, J., Deng, B., Polymer-matrix nanocomposite membranes for water treatment. *J. Membr. Sci.* 2015, 479, 256-275.

45. Bashir, T., Department of Chemical and Biological Engineering, School of Engineering, CHALMERS UNIVERSITY OF TECHNOLOGY UNIVERSITY OF BORÅS, Chalmers University of Technology, Göteborg, Sweden 2013, p. 65.
46. Xue, C.-H., Chen, J., Yin, W., Jia, S.-T., Ma, J.-Z., Superhydrophobic conductive textiles with antibacterial property by coating fibers with silver nanoparticles. *Appl. Surf. Sci.* 2012, 258, 2468-2472.
47. Yuan, C., Hou, L., Li, D., Shen, L., et al., Synthesis of flexible and porous cobalt hydroxide/conductive cotton textile sheet and its application in electrochemical capacitors. *Electrochim. Acta* 2011, 56, 6683-6687.
48. Wiener, J., Ramadan, M., Gomaa, R., Abbasi, R., Hebeish, A., Preparation and Characterization of Conductive Cellulosic Fabric by Polymerization of Pyrrole. *Materials Sciences and Applications* 2013, 04, 649-655.
49. Abbasi, A. M. R., Ramadan, M. A., Wiener, J., Baheti, V., Militky, J., Electrothermal feedback in polypyrrole coated cotton fabric. *Journal of Textile Engineering* 2013, 59, 93-98.
50. Ramadan, M. A. M., Fathi, A., Shaarawy, S., El-bisi, M., A New Approach for Preparation of Smart Conductive Textiles by Polyaniline through in-situ Polymerization Technique. *Egypt. J. Chem.* 2018, 61, 479-492.
51. Ramadan, M., Abbasi, R., Wiener, J., Baheti, V., Militky, J., Polypyrrole coated cotton fabric: The thermal influence on conductivity. *Vlakna a Textil* 2012, 19, 41-49.
52. Mäkelä, T., Jussila, S., Vilkmann, M., Kosonen, H., Korhonen, R., Roll-to-roll method for producing polyaniline patterns on paper. *Synth. Met.* 2003, 135-136, 41-42.
53. Trey, S., Jafarzadeh, S., Johansson, M., In situ polymerization of polyaniline in wood veneers. *ACS Applied Materials and Interfaces* 2012, 4, 1760-1769.
54. Qaiser, A. A., Hyland, M. M., Patterson, D. A., Surface and Charge Transport Characterization of Polyaniline-Cellulose Acetate Composite Membranes. *The Journal of Physical Chemistry B* 2011, 115, 1652-1661.
55. Rodríguez, F., Castillo-Ortega, M. M., Encinas, J. C., Grijalva, H., et al., Preparation, characterization, and adsorption properties of cellulose acetate-polyaniline membranes. *J. Appl. Polym. Sci.* 2009, 111, 1216-1224.
56. Devasenan, S., Hajara Beevi, N., Jayanthi, S. S., Synthesis and characterization of silver nanoparticles by chemical reduction method and their antimicrobial activities. *International Journal of ChemTech Research* 2016, 9, 571-576.
57. Kheawhom, S., Panyarueng, P., Synthesis and Characterization of Copper-Silver Core-Shell Nanoparticles by Polyol Successive Reduction Process. *Materials Research Society Symposia Proceedings* 2014, 1630, 1-4.
58. Mlambo, M., Mdluli, P. S., Shumbula, P., Skepu, A., et al., A size-controlled synthesis and characterization of mixed monolayer protected silver-S-(CH<sub>2</sub>)<sub>11</sub>-NHCO-coumarin nanoparticles and their Raman activities. *J. Mater. Res.* 2015, 30, 1934-1942.
59. Zheng, Y., Chen, S., Wang, S., Song, X., Hu, S., Synthesis and Antibacterial Property of Colloidal Silver Dispersed in Anhydrous Glycerin. *Cailiao Daobao/Materials Review* 2017, 31, 30-34.
60. Malik, P., Inwati, G. K., Mukherjee, T. K., Singh, S., Singh, M., Green silver nanoparticle and Tween-20 modulated pro-oxidant to antioxidant curcumin transformation in aqueous CTAB stabilized peanut oil emulsions. *J. Mol. Liq.* 2019, 291, 111252.
61. Peddi, S. P., Sadeh, B. A., *IOP Conference Series: Materials Science and Engineering* 2015.
62. Desai, R., Mankad, V., Gupta, S. K., Jha, P. K., Size Distribution of Silver Nanoparticles: UV-Visible Spectroscopic Assessment. *Nanoscience and Nanotechnology Letters* 2012, 4, 30-34.
63. Liebeck, B. M., Hidalgo, N., Roth, G., Popescu, C., Boker, A., Synthesis and Characterization of Methyl Cellulose/Keratin Hydrolysate Composite Membranes.

- Polymers (Basel) 2017, 9, 1-13.
64. El-Sheikh, M. A., Chemistry (Easton), Faculty of Science, Cairo University, Egypt 1999, pp. 43-96.
  65. Chen, C., Wang, L., Jiang, G., Zhou, J., et al., Study on the synthesis of silver nanowires with adjustable diameters through the polyol process. *Nanotechnology* 2006, 17, 3933-3938.
  66. Gupta, K., Jana, P. C., Meikap, A. K., Optical and electrical transport properties of polyaniline-silver nanocomposite. *Synth. Met.* 2010, 160, 1566-1573.
  67. Khandelwal, M., Kumar, A., One-pot environmentally friendly amino acid mediated synthesis of N-doped graphene-silver nanocomposites with an enhanced multifunctional behavior. *Dalton Trans* 2016, 45, 5180-5195.
  68. Singh, R. P., Tiwari, A., Pandey, A. C., Silver/Polyaniline Nanocomposite for the Electrocatalytic Hydrazine Oxidation. *Journal of Inorganic and Organometallic Polymers and Materials* 2011, 21, 788-792.
  69. Tamboli, M. S., Kulkarni, M. V., Patil, R. H., Gade, W. N., et al., Nanowires of silver-polyaniline nanocomposite synthesized via in situ polymerization and its novel functionality as an antibacterial agent. *Colloids Surf. B. Biointerfaces* 2012, 92, 35-41.
  70. Sukhanova, T. E., Santuryan, Y. G., Alekseeva, P. E., Valueva, S. V., et al., Bioactive Silver-Containing Compositions of Methyl Cellulose with a Natural Sorbent Zosterin: The Structure, Morphology, and Properties. *Technical Physics* 2018, 63, 1420-1426.